Title: Data to support Structural Consequences of Different Metal Compositions in the Doped Spin-Crossover Crystals $[Fe_zM_{1-z}(bpp)_2][BF_4]_2$ (M = Ni, Zn; bpp = 2,6-Bis{pyrazol-1-yl}pyridine).

Creator(s): Christopher M. Pask,[1] Alexander N. Kulak[1] and Malcolm A. Halcrow[1]

Organisation(s): 1. University of Leeds, UK.

Publication Year: 2024

Description: Variable temperature crystallographic characterization of $[Fe_zZn_{1-z}(bpp)_2][BF_4]_2$ (bpp = 2,6-*bis*{pyrazol-1-yl}pyridine*; z* = 0.88, 0.69 and 0.27) and $[Fe_zNi_{1-z}(bpp)_2][BF_4]_2$ (*z* = 0.83, 0.72 and 0.30) is presented. Comparison with previously published data confirms the isothermal unit cell volume change during spin-crossover (ΔV_{SCO}) behaves differently in the Zn- and Ni-doped crystals. For the FeZn crystals, the relationship between ΔV_{SCO} and *z* is approximately linear for $z \geq 0.4$ but is steeper than expected, so $\Delta V_{SCO} \approx 0$ for *z* = 0.27. In contrast the same correlation in the FeNi materials is non-linear, with ΔV_{SCO} varying only slightly between $0.83 \geq z \geq 0.46$ before decreasing more strongly at higher dilution. Moreover ΔV_{SCO} in each FeZn crystal is smaller than for its FeNi analogue with a similar composition. As well as the dopant ion ionic radius, the smaller ΔV_{SCO} for the Zn-doped materials reflects their lower $T_{½}$ values compared to their FeNi counterparts, which is especially evident at high metal dilution.

Cite as: Pask, Christopher M., Kulak, Alexander N., and Halcrow, Malcolm A. (2024). Data to support Structural Consequences of Different Metal Compositions in the Doped Spin-Crossover Crystals $[Fe_zM_{1-z}(bpp)_2][BF_4]_2$ (M = Ni, Zn; bpp = 2,6-Bis{pyrazol-1-yl}pyridine). University of Leeds. [Dataset] https://doi.org/10.5518/1540

Related publication: Pask, Christopher M., Kulak, Alexander N., and Halcrow, Malcolm A. (2024). Data to support Structural Consequences of Different Metal Compositions in the Doped Spin-Crossover Crystals $[Fe_zM_{1-z}(bpp)_2][BF_4]_2$ (M = Ni, Zn; bpp = 2,6-Bis{pyrazol-1-yl}pyridine). *European Journal of Inorganic Chemistry*, doi: 10.1002/ejic.202400334.

Contact: m.a.halcrow@leeds.ac.uk

2. TERMS OF USE

3. PROJECT AND FUNDING INFORMATION

n/a

4. CONTENTS

The dataset contains data for this study:

Scanning Electron Microscopy images and EDX element maps (*EDX*.zip)

X-ray Crystallographic data (*crystal*.zip):

- Structure of **1a** at 100 K (CCDC 2359124)
- Structure of **1a** at 300 K (CCDC 2359125)
- Structure of **1b** at 100 K (CCDC 2359126)
- Structure of **1b** at 300 K (CCDC 2359127)
- Structure of **1d** at 100 K (CCDC 2359128)
- Structure of **1d** at 300 K (CCDC 2359129)
- Structure of **2a** at 100 K (CCDC 2359130)
- Structure of **2a** at 300 K (CCDC 2359131)
- Structure of **2b** at 100 K (CCDC 2359132)
- Structure of **2b** at 300 K (CCDC 2359133)
- Structure of **2d** at 100 K (CCDC 2359134)
- Structure of **2d** at 300 K (CCDC 2359135)
- Variable temperature unit cell data for **1a**
- Variable temperature unit cell data for **1b**
- Variable temperature unit cell data for **1d**
- Variable temperature unit cell data for **2a**
- Variable temperature unit cell data for **2b**
- Variable temperature unit cell data for **2d**

Linear thermal expansion coefficient calculations (*PASCal* outputs – *LTE*.zip)

5. METHODS

Full details are provided in the related publication, listed above.

Compounds referred to in this dataset

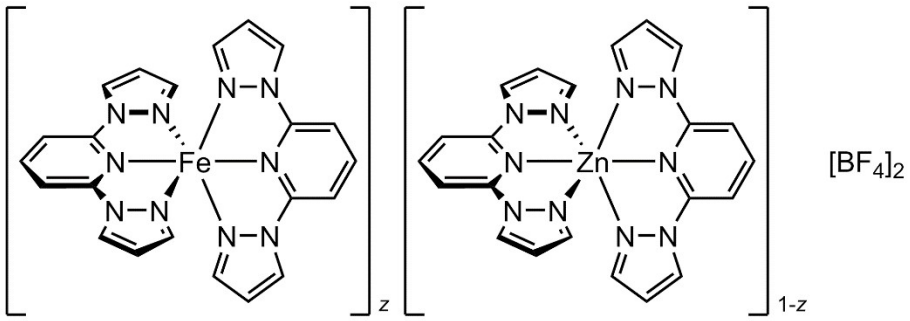

$[Fe_zZn_{1-z}(bpp)_2][BF_4]_2$
Bis[di(pyrazol-1-yl)pyridine]iron(II):zinc(II) di(tetrafluoroborate) solid solution
$C_{22}H_{18}B_2F_8Fe_zN_{10}Zn_{1-z}$
z = 0.88, **1a**
z = 0.72, **1b**
z = 0.54, **1c**
z = 0.27, **1d**

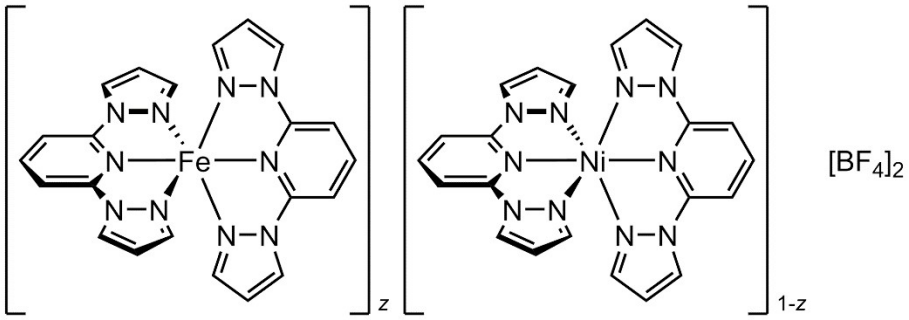

$[Fe_zNi_{1-z}(bpp)_2][BF_4]_2$
Bis[di(pyrazol-1-yl)pyridine]iron(II):nickel(II) di(tetrafluoroborate) solid solution
$C_{22}H_{18}B_2F_8Fe_zN_{10}Ni_{1-z}$
z = 0.83, **2a**
z = 0.72, **2b**
z = 0.46, **2c**
z = 0.32, **2d**